Arch Biol Sci. 2024;76(4):409-418 https://doi.org/10.2298/ABS240812031S

ABA enhances the apoptotic effect of docetaxel in the multidrug-resistant DU145 prostate cancer cell line

Deniz Şumnulu[1,*] and Zeynep Banu Doğanlar[2]

[1]*Technology Research Development Application and Research Centre, Trakya University*, Edirne, Turkey
[2]*Faculty of Medicine, Department of Medical Biology, Trakya University*, Edirne, Turkey

***Corresponding author**: denizsumnulu@trakya.edu.tr

Received: August 12, 2024; **Revised**: September 20, 2024; **Accepted**: October 9, 2024; **Published online**: October 18, 2024

Abstract: This study aimed to induce drug resistance in DU145 prostate cancer cells by exposing them to docetaxel and mitoxantrone, and to examine the effects of combining docetaxel and abscisic acid (ABA). The IC_{50} values for docetaxel and mitoxantrone in non-resistant cells were 54.57 nM and 6.25 nM, respectively, rising to 808.53 nM and 50.07 nM after resistance had developed. RT-PCR analysis showed that treatment of resistant cells with 50.07 nM docetaxel and 500 μM ABA (ABA) resulted in the following changes in gene expression: heat shock protein (HSP) 70 (0.63-fold), glucose-regulated protein 94 (GRP94) 0.33-fold, inositol-requiring transmembrane kinase endoribonuclease-1α (IRE1α) 1.62-fold, ER degradation-enhancing alpha-mannosidase-like 1 (EDEM1) 1.77-fold, X-box binding protein 1 (XBP1) 1.53-fold, p21 (2.53-fold), cellular tumor antigen p53 (p53) 2.49-fold, bcl-2-like protein 4 (Bax) 2.7-fold, and tumor necrosis factor (TNF-α) 6.35-fold. Tali™ cytometry analysis showed a 47% increase in apoptotic/necrotic cells with the combined treatment of docetaxel and ABA, compared to a 26% increase with docetaxel alone. Fluorescent staining revealed that co-administration of docetaxel and ABA increases apoptosis in resistant DU145 cells compared to treatment with docetaxel alone. This study suggests that combining ABA with docetaxel could be effective in drug-resistant prostate cancer.

Keywords: ABA, docetaxel, drug resistance, HSP70, GRP94

INTRODUCTION

Cancer is a major health threat, with 20 million new cases reported in 2022. Both the Food and Drug Administration (FDA) and the European Medicines Agency (EMA) have approved a wide range of anticancer drugs [1]. Despite advancements, many of these drugs continue to face significant challenges, such as high systemic toxicity from poor tumor selectivity and pharmacokinetic limitations like low water solubility, which can reduce their circulation time [2]. Additionally, cancer cells often develop resistance to these treatments, either over time or after a short period of use [3,4].

Certain cancers, such as non-small cell lung cancer and colon cancer, exhibit resistance to chemotherapy drugs from the outset [3,4]. The initial treatment strategy for metastatic prostate cancer involves androgen hormone deprivation, which can lead to the development of castration-resistant prostate cancer (CRPC). Docetaxel, a taxane drug that stabilizes microtubules to exert its cytotoxic effects, is frequently used to treat metastatic CRPC [5]. However, resistance to docetaxel remains a significant challenge, impacting nearly half of all patients [6-8]. This resistance is typically caused by factors such as the activation of multiple drug resistance (MDR) genes, leading to decreased drug uptake, and the activation of alternative growth pathways that counteract the effects of docetaxel [9,10].

To tackle these challenges, a common approach is to combine docetaxel with other agents, such as mitoxantrone, a synthetic anthracenedione that inhibits DNA topoisomerase II [11-13]. Mitoxantrone also exhibits a high cytotoxic effect not only on cancer cell lines but also on healthy cell lines [14-17]. As a result, overcoming multidrug resistance (MDR) remains a crucial focus in cancer research [18].

Abscisic acid (ABA) is an important phytohormone responsible for abiotic stress tolerance in plants [19, 20]. By inducing dormancy in plants during stressful conditions such as drought, high temperatures, or excessive soil salinity, ABA protects them from potential damage [20]. Studies have shown that the signaling pathway triggered by ABA regulates chaperone proteins such as HSP70 and HSP90, which function as co-chaperones to counteract reactive oxygen species (ROS) generated by environmental stresses. Moreover, studies have demonstrated that ABA is also produced by hematopoietic immune cells, including mammalian pancreatic β cells, adipocytes, keratinocytes, granulocytes, monocytes, and macrophages, as well as human mesenchymal stem cells, and it is found in blood plasma [21,22]. Similar to its effects in plants, a study reported that applying ABA to the PC3 prostate cancer cell line at a dose of 50 μM for 72 h induced dormancy by arresting the cells in the G_0 phase of the cell cycle [23]. Furthermore, a study conducted on a glioma cell line demonstrated that ABA induces apoptosis by inhibiting the activity of peroxisome proliferator-activated receptors (PPARs). This finding suggests that ABA can influence cell death mechanisms through the modulation of PPAR activity, highlighting its potential as a therapeutic agent in cancer treatment [24].

In this study, we aimed to develop multiple drug resistance in the DU145 prostate cancer cell line by applying effective doses of docetaxel and mitoxantrone through serial passaging. The research also planned to explore the molecular mechanisms of combining docetaxel, an FDA-approved drug for treating prostate cancer, with ABA, a naturally occurring plant and human hormone, to combat the induced drug resistance.

MATERIALS AND METHODS

Ethics statement

Cells cultured *in vitro* were used. No human subjects or animals were involved at any stage of the research.

Cell culture

The DU145 prostate cancer cell line (ATCC ® HTB-81™) was sourced from the American Type Culture Collection (ATCC® HTB-81™, USA). Cells were grown in Dulbecco's Modified Eagle's Medium/Nutrient F-12 Ham (Multicell, Canada), supplemented with 5% fetal bovine serum (FBS; SIGMA-ALDRICH, USA), and 1% L-glutamine (Thermo Fisher Scientific, USA) was used as the culture medium. To prevent bacterial and fungal contamination, 100 IU/mL penicillin-streptomycin (Pen-Strep; Thermo Fisher Scientific) and 100× antibiotic-antimycotic (Gibco, Thermo Fisher Scientific) were added. Cells were incubated at 37°C in a 5% CO_2 environment. Passaging was performed approximately every 48 h once the cells reached 90% confluence.

Cell viability assays

The cell viability tetrazolium dye or 3-(4,5-dimethylthiazol-2-yl)-2,5-diphenyltetrazolium bromide (MTT) assay [25] was used to determine the optimal concentrations and durations of docetaxel, mitoxantrone, and ABA for the DU145 cell line. Initially, 5×10^3 cells were seeded into each well of transparent spectrophotometric 96-well plates and incubated at 37°C in 5% CO_2 for 24 h. After the incubation period, the DU145 cell line was treated with docetaxel concentrations ranging from 0.39 to 200 nM, combined concentrations of docetaxel and mitoxantrone ranging from 0.39 to 100 nM each, and ABA concentrations from 3.9 μM to 2 mM. The treatment durations were 24, 48, and 72 h. Each treatment was performed in triplicate. After the treatment periods, 20 μL of MTT solution (0.5 mg/mL; Biomatik, USA) was added to each well and incubated for 2 h. Subsequently, the liquid phase was removed, and 180 μL of dimethyl sulfoxide (DMSO) was added to each well. Cell viability was then assessed by measuring the absorbance at 570 nm using a Multiskan GO plate reader (Thermo Fisher Scientific).

Light microscopy assays

Concentrations ranging from 0.39 to 100 nM of both docetaxel and mitoxantrone in combination were applied to both non-resistant (NR) DU145 and resistance-induced (DR) DU145 cell lines for 72 hours. Changes in cell quantities were compared using a light microscope (Nikon ECLIPSE TS100, Japan) with a 10× objective for comparative analysis.

Apoptosis assays

Apoptosis was assessed via the detection of damage to nuclear and cell membrane structures. Cells (5×10^4) were seeded into each well of 24-well plates with 0.5 mL of culture medium. The half-maximal inhibitory concentration (IC_{50}) dose of docetaxel for non-resistant DU145 (NR_DU145) cells was determined over 72 h, and this NR_DU145 dose was combined with the highest cytotoxic dose of ABA applied for 48 h to the resistance-induced DU145 (DR_DU145) cell line. After the treatments, the liquid phase in the wells was removed. To visualize apoptosis in the nuclei, 10 µL of NucBlue™ Live ReadyProbes™ Reagent (Thermo Fisher Scientific, USA) diluted in phosphate buffer saline (PBS) were added. To assess the changes in membrane structure due to early apoptosis and cytoskeletal disruption, 10 µL of caspase 3/7 reagent (Thermo Fisher Scientific, USA), also dissolved in PBS, was used. For detecting late apoptosis and necrosis, 10 µg/mL of acridine orange (AO) and 10 µg/mL of ethidium bromide (EB) dissolved in PBS were applied. All dyes were incubated with the cells in the dark at room temperature for 30 min. Following incubation, cells labeled with NucBlue™ were imaged on the fluorescent stain 4',6-diamidino-2-phenylindole (DAPI) channel, those labeled with caspase 3/7 were imaged on the fluorescein isothiocyanate (FITC) channel, and cells labeled with AO and EB were imaged on the RED channel, all with a 20× objective of a fluorescence microscope (Observer Z1, ZEISS, Germany).

The DR_DU145 cells were seeded at 5×10^5 cells per 25 cm^2 flask for three groups: the control group, the NR_Dose application group, and the group receiving a combination of NR_Dose and the highest cytotoxic dose of ABA. Each treatment was conducted in triplicate. At the end of each treatment duration, cells were trypsinized by centrifugation at 800 ×g for 2.5 min at 4°C. For percentage comparison of viable, apoptotic, and necrotic cells, the Tali® Apoptosis Kit (Life Technologies) was utilized. The cell pellet was resuspended in 100 µL of Annexin V binding buffer mixed with 5 µL Annexin V Alexa Fluor® 488, and 5 µL Tali® Propidium Iodide (PI). After 25 min incubation at room temperature and in the dark, the cells were loaded onto Tali® cellular analysis slides in a volume of 25 µL. The Tali™ Image-Based Cytometer (Invitrogen) software was used to count live, dead, and apoptotic cells.

RNA extraction and cDNA synthesis

The NR_Dose, NR_Dose+$ABA_{500\mu M}$, and 6.25 nM docetaxel-mitoxantrone treatment and control groups were trypsinized and collected by centrifugation at 10000 ×g for 1 min. RNA isolation was performed using an RNA isolation kit (Ambion Life Technologies, Invitrogen, Thermo Fisher Scientific) following the provided protocol. The quantity of isolated RNA was measured by spectrophotometry (OPTIZEN NanoQ, Republic of Korea). The RNA quantities in the various samples were adjusted using deionized water (dH_2O), and cDNA was synthesized with a reverse transcription kit (Invitrogen, USA). The cDNA synthesis was carried out in a thermal cycler (Applied Biosystems, USA), using the following protocol: 10 min at 25°C, 120 min at 37°C, and 5 min at 85°C.

Quantitative real time PCR (qRT-PCR)

qRT-PCR analysis was used to investigate changes in the expression levels of selected genes. Sequences of the primers used to amplify corresponding transcripts are given in Supplemental Table S1. The 18S gene served as an internal reference. The PCR amplification was performed using an ABI StepOne™ RT-PCR instrument (Applied Biosystems, Thermo Fisher Scientific) as follows: initial denaturation at 95°C for 10 min, followed by 40 cycles of denaturation at 95°C for 10 s, annealing at 50°C for 2 min, and extension at 60°C for 1 min.

Statistical analysis

Cell viability calculations following treatments were performed using the formula:

Cell viability (%)=(absorbance value for wells with treated cells / absorbance value for wells with control cells)×100

The IC_{50} of the NR_DU145 and DR_DU145 cell lines were determined using the SPSS Regression Probit application (IBM SPSS Statistics 22). Changes in gene expressions were calculated using the $2^{-\Delta\Delta CT}$ formula. Comparisons of gene expression levels among two groups were analyzed using the SPSS Paired Samples t test. Comparisons of gene expression levels among multiple groups and the quantities of live, apoptotic, and dead cells from Tali imaging-based cytometric

analyses were conducted using one-way ANOVA with Tukey's post-hoc HSD test in SPSS (IBM SPSS Statistics 22.0). Statistical significance was considered at $P<0.05$.

RESULTS

Development of drug resistance in DU145 prostate cancer cell line

Both docetaxel alone and the docetaxel-mitoxantrone combination were the most effective when cells were treated for 72 h. We determined the IC_{50} value for docetaxel to be 54.57 nM, while the IC_{50} for the combined treatment of 6.25 nM docetaxel and 6.25 nM mitoxantrone after 72 h was also calculated. The NR_DU145 cell line developed drug resistance over 25 passages with the docetaxel-mitoxantrone combination. No application was made during the following five passages to assess whether the resistance of DU145 cells was permanent. The MTT test was performed on the cells with different doses of docetaxel and the docetaxel-mitoxantrone combination to determine new IC_{50} after the 5th passage. Results of the MTT test revealed that the new IC_{50} value for docetaxel alone was 808.53 nM, while for the combined treatment with docetaxel and mitoxantrone the IC_{50} value was 50.07 nM.

Due to its high cytotoxicity on both cancerous and healthy cells, mitoxantrone was utilized solely while developing drug resistance in the DU145 cell line. After inducing MDR in the DU145 cell line, we attempted to overcome this resistance by applying docetaxel at its IC_{50} dose for the NR_DU145 cell line, along with ABA at its highest effective dose for the DR_DU145 cell line. When DR_DU145 cells were treated with ABA at concentrations ranging from 3.9 µM to 2 mM for 24, 48, and 72 h, the most effective treatment duration was 48 h. Their viability was 74.78±2.24% compared to control DR_DU145 cells when 500 µM ABA was used for 48 h. Conversely, the viability of DR_DU145 cells increased when 1 mM (77.95±2.33%) or 2 mM ABA (78.48±3.64%) was used. Therefore, for downstream application, DR_DU145 cells were treated with 500 µM ($ABA_{500\mu M}$) for 48 h.

Drug resistance of the DU145 cell line resulting from the combined application of 6.25 nM of docetaxel and 6.25 nM of mitoxantrone for 72 h over 25 passages was demonstrated by the higher viable cell count in the resistant DR_DU145 cell line compared to the non-resistant NR_DU145 cell line. This was also evident in drug resistance when lower and higher (0.39-100 nM) doses of docetaxel and mitoxantrone were combined and applied to both cell lines for 72 h (Fig. 1).

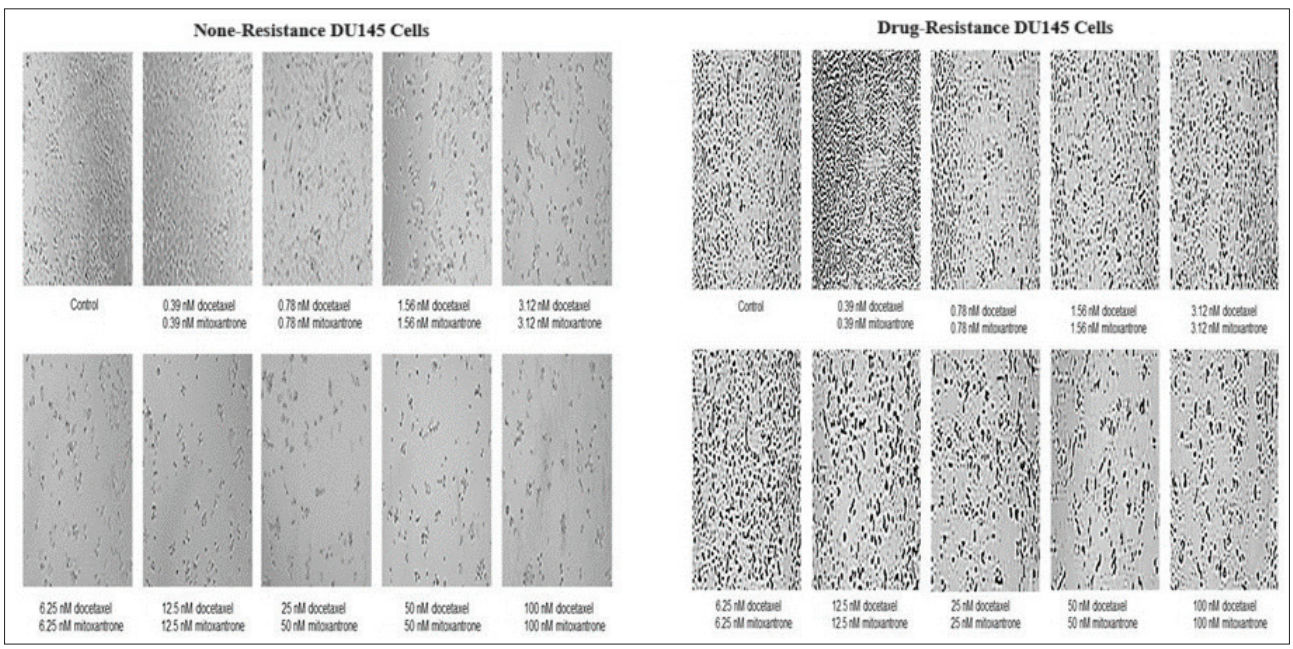

Fig. 1. Cell number changes after combined application of 0.39-100 nM docetaxel and 0.39-100 nM mitoxantrone to the non-resistant and multidrug-resistant DU145 cell lines.

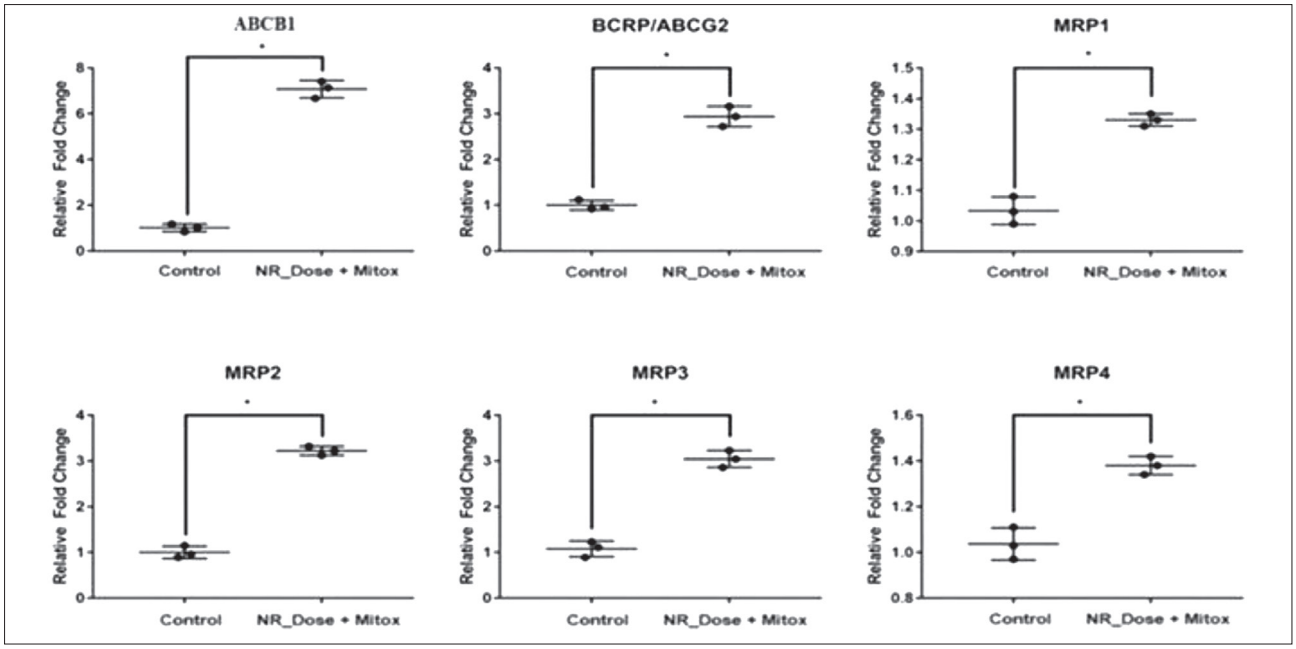

Fig. 2. Changes in drug resistance gene expression levels in DR_DU145 cell line following the combined application of 6.25 nM docetaxel-mitoxantrone (n=3±SD) (*P<0.05).

To assess whether drug resistance of the DR_DU145 cell line developed by serial administrations of docetaxel and mitoxantrone affects the expression levels of drug resistance genes, qRT-PCR was used to amplify multidrug resistance protein 1 (MDR1) or ATP-binding cassette sub-family B member 1 (ABCB1) (7.07±0.4), breast cancer resistance protein (BCRP)/ATP-binding cassette subfamily G member 2 (ABCG2) BCRP/ABCG2 (2.94±0.22), MDR proteins (MRP) -1 (1.33±0.2), MRP2 (3.22±0.1), MRP3 (3.04±0.18), and MRP4 (1.38±0.04) transcripts from cells treated with 6.25 nM docetaxel-mitoxantrone combination. These changes are illustrated in Fig. 2.

ABA increases apoptosis in the DR_DU145 cell line treated with docetaxel

To assess how ABA affects DR_DU145 cells, the cells were treated with an IC_{50} dose of docetaxel determined for the NR_Dose and the combination of NR_Dose with $ABA_{500\mu M}$. Changes in the expression levels of genes related to apoptosis, including HSP70, GRP94, PERK, Ire1-α, EDEM1, XBP1, p21, p53, Bax, and TNF-α were determined by qPCR. Results obtained for three groups (control, NR_Dose and NR_Dose+$ABA_{500\mu M}$) were compared. While there were significant increases in the expression levels of HSP70, GRP94, and PERK genes in the DR_DU145 cell line in response to NR_Dose treatment compared to the control, there were significant decreases in HSP70 and GRP94 gene expressions in response to the NR_Dose+$ABA_{500\ \mu M}$ treatment compared to both the control and NR_Dose treatment. Additionally, for the NR_Dose+$ABA_{500\mu M}$ treatment, significant increases were observed in the expression levels of PERK, Ire1-α, EDEM1, XBP1, p21, p53, Bax, and TNF-α genes. The expression levels are detailed in Table 1.

Table 1. Changes in gene expression levels in the DR_DU145 cell line following the application of NR_Dose and NR_Dose+$ABA_{500\mu M}$.

Genes	DR_DU145 cell line relative expression level changes		
	NR_Dose to Control	NR_ Dose+$ABA_{500\mu M}$ to Control	NR_ Dose+$ABA_{500\mu M}$ to NR_Dose
HSP70	1.34*±0.1	-0.3*±0.08	-1.64*±0.07
GRP94	0.85*±0.2	-0.69*±0.16	-1.54*±0.1
PERK	0.59*±0.22	1.39*±0.22	0.79*±0.16
Ire1-α	-0.007^{ns}±0.27	0.6*±0.2	0.61*± 0.07
EDEM1	0.02^{ns}±0.08	0.77*±0.27	0.75*±0.18
XBP1	0.01^{ns}±0.15	0.88*±0.24	0.87*±0.15
p21	-0.003$^{ns±}$0.06	1.52*±0.15	1.52*±0.15
p53	0.08^{ns}±0.18	0.79*±0.12	0.71*±0.17
Bax	-0.08^{ns}±0.09	1.73*±0.14	1.81*±0.2
Tnf-α	0.13^{ns}±0.17	5.44*±0.36	5.31*±0.38
n=3±SD (^{ns}P>0.05, *P<0.05).			

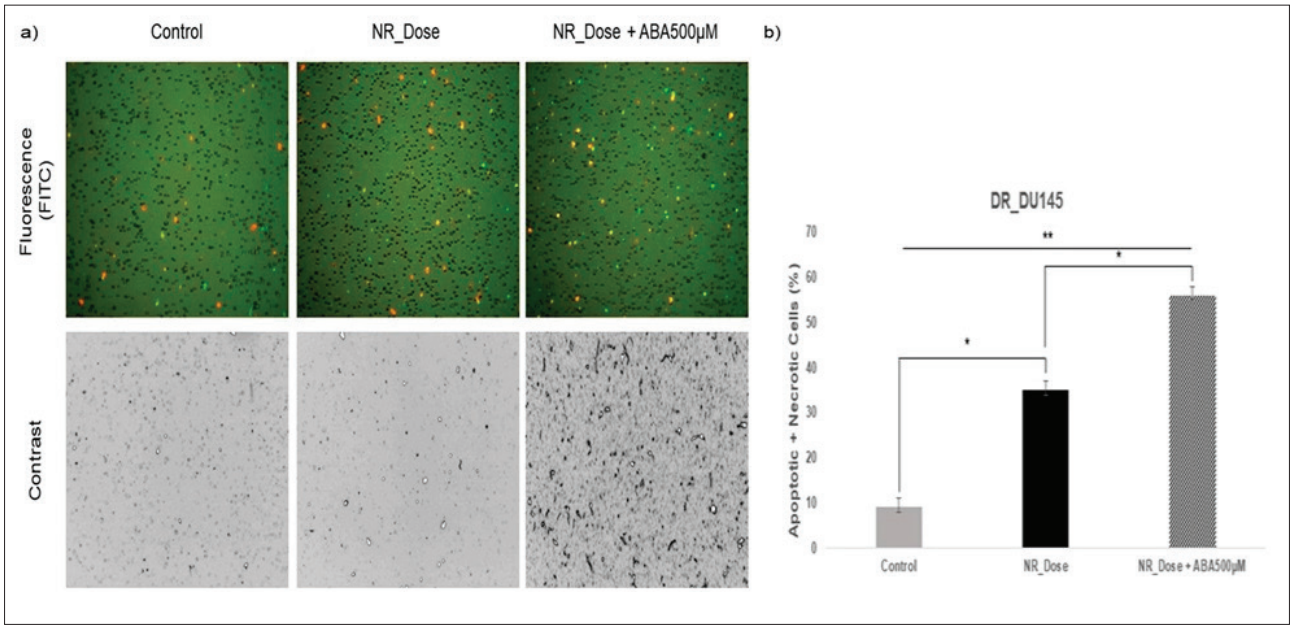

Fig. 3. Comparison of viable, apoptotic, and dead DR_DU145 cell counts following treatments with docetaxel and ABA. **A** – Fluorescence image; dead cells labeled with PI appear red, apoptotic cells labeled with Annexin-V appear green, and unaffected live cells appear black. **B** – Comparison of total apoptotic and necrotic cells between control and treatment groups (n=3±SD) (*p<0.05, **p<0.01).

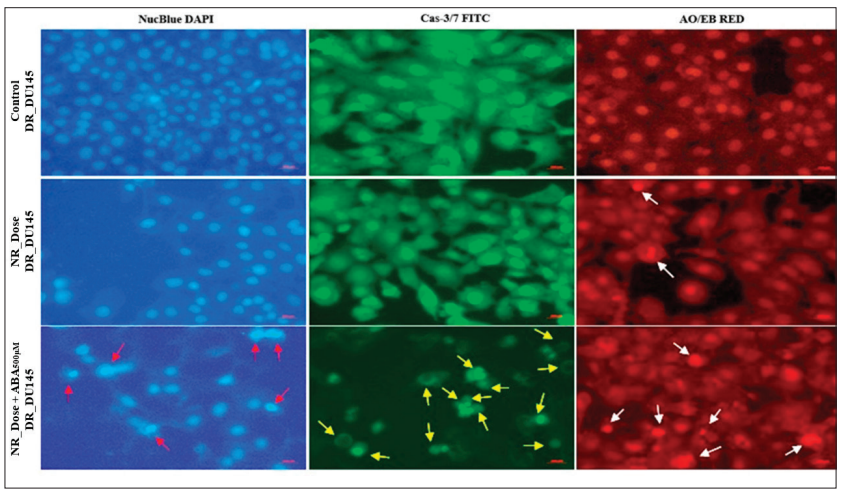

Fig. 4. Comparison of changes in nuclear and membrane structures in fluorescence-labeled DR_DU145 cell line following NR_Dose and NR_Dose+$ABA_{500\mu M}$ applications compared to control. Red arrows indicate nuclear damage, yellow arrows indicate skeletal damage, white arrows indicate both nuclear and skeletal damage in DR_DU145 cells.

We counted apoptotic and dead DR_DU145 cells after the co-treatment with docetaxel and ABA. Application of NR_Dose of docetaxel resulted in a 26±2.3% increase in total apoptotic and dead cell counts compared to the control untreated DR_DU145 cells. In contrast, the co-application of NR_Dose+$ABA_{500\mu M}$ led to a 47±2.1% increase in these cell counts compared to the control. Furthermore, NR_Dose+$ABA_{500\mu M}$ co-application resulted in a 21±3.6% increase in total apoptotic and dead cell counts compared to NR_Dose alone. These differences were statistically significant among the groups (Fig. 3).

In the DR_DU145 cell line, although no disruptions in the cytoskeletal structure, an early apoptosis marker, were observed in response to the NR_Dose treatment compared to the control, a few fluorescent signals were detected due to nuclear structural abnormalities, which are indicators of late apoptosis. In contrast, in response to the NR_Dose+$ABA_{500\mu M}$ treatment, the cytoskeletal structure of DR_DU145 cells took on a spherical shape and fluorescent signals were detected due to nuclear structural abnormalities. These changes are demonstrated in Fig. 4.

DISCUSSION

The development of drug resistance over time to docetaxel, a primary therapeutic agent for prostate cancer, and the adjunct chemotherapeutic agent

mitoxantrone, as reported in [6,7], was induced in the DU145 prostate cancer cell line following the combined application of these two drugs. The developed drug resistance was demonstrated through MTT analysis, which showed that the IC_{50} value increased approximately 14.82-fold compared to the NR_DU145 cell line following docetaxel application, and about 8-fold following the combined application of docetaxel and mitoxantrone. Light microscopy imaging revealed a higher reduction in cell proliferation in the NR_DU145 cell line compared to the DR_DU145 cell line after increasing doses of combined docetaxel-mitoxantrone were applied.

Furthermore, qRT-PCR analyses indicated significant increases in the expression levels of the ABCB1, BCRP, MRP1, MRP2, MRP3, and MRP4 genes in the DR_DU145 cell line following the combined application of docetaxel and mitoxantrone. In prostate cancer, the increased expression of ABCB1, BCRP/ABCG2, and various MRP genes in response to mitoxantrone treatment is a key mechanism that contributes to drug resistance [26]. Additionally, overexpression of the ABCB1 gene is a recognized feature in prostate cancer types resistant to docetaxel [27]. Moreira et al. (2021) observed a significant increase in ABCB1 gene expression following serial passaging in C4-2B and LNCaP prostate cancer cell lines treated with docetaxel [28].

After developing MDR in the DR_DU145 prostate cancer cell line, we investigated the apoptotic effects by combining docetaxel with ABA to reverse the effects of resistance, particularly against docetaxel. Given the high degree of hepatotoxicity associated with mitoxantrone compared to docetaxel [29], mitoxantrone was omitted from the subsequent stages of the study; it was only utilized to induce MDR.

The GRP94, a member of the mammalian HSP90 family, functions within the secretory pathway to ensure proper protein folding in the endoplasmic reticulum (ER) [30]. Unlike co-chaperones, GRP94 acts as a chaperone protein by binding to the adenosine triphosphate BiP, a constitutively expressed resident protein in the ER and a subunit of HSP70 under harsh denaturation conditions, thereby enhancing the expression of HSP70. This process aids in the refolding of misfolded proteins, thereby mitigating potential ER stress [31].

In this study, an increase in the expression levels of chaperone proteins, specifically HSP70 and GRP94, was observed in the DR_DU145 cell line in response to docetaxel application. A significant increase in expression was also noted for the ER stress gene PERK, while the levels of Ire1-α, EDEM1, and XBP1 remained unchanged. No significant changes were observed in the expression levels of apoptotic and necrotic genes such as p21, p53, Bax, and TNF-α.

In mammals, the induction of XBP1 is primarily associated with increased expression of PERK, IRE1-α, EDEM1, and especially GRP94, due to the accumulation of unfolded or misfolded proteins in the ER. This leads to either a halt in ER protein synthesis to alleviate stress or cell apoptosis if stress is excessive [32]. The significant increase in PERK expression, combined with stable levels of other ER stress response genes and apoptotic/necrotic genes suggests an overall suppression of stress.

Conversely, in the DR_DU145 cell line, combined docetaxel and ABA application resulted in significant decreases in HSP70 and GRP94 expression levels compared to both the control and docetaxel application groups. This reduction in HSP gene expression in response to ER stress indicates an upregulation of PERK, IRE1-α, EDEM1, and XBP1 genes. The increased ER stress led to a notable rise in TNF-α expression levels, which triggered the p21 gene and caused cell cycle arrest at the G1 phase. This cell cycle arrest subsequently resulted in increased expression of the p53 gene, which activated the pro-apoptotic gene Bax, leading to apoptosis in DR_DU145 cells. Similarly, Akashi et al. demonstrated that TNF-α application in WiDr human colon cancer cells increased the expression of p21, p53, and Bax, leading to apoptosis [33].

Additionally, Tali cytometer analyses revealed a significant increase in apoptotic and necrotic cell numbers in the DR_DU145 cells following combined docetaxel and ABA application compared to the control and docetaxel application groups. Fluorescence microscopy further confirmed that docetaxel and ABA application disrupted the cell cytoskeleton, leading to spherical cell morphology and the appearance of fluorescence indicative of late apoptosis/necrosis in the nucleus. These findings show that 500 μM of ABA significantly enhances the cytotoxic effect of docetaxel on the DR_DU145 cell line.

Numerous studies in plants have demonstrated that ABA (ABA), particularly when secreted in response to heat stress, triggers the expression of HSP70. This process promotes dormancy by mitigating the effects of ROS [34-36]. Additionally, research by Taichman et al. [22] has shown that ABA increases the expression of TNF-α, p21, and p27 in LNCaP prostate adenocarcinoma cells, the PC3 prostate cancer cell line, and DU145 cells. The authors found that elevated p21 expression leads to PPAR γ receptor signal activation and cell cycle arrest at the G0 phase and entry into dormancy.

In contrast to previous studies, which indicated that ABA promotes the expression of HSP70 and HSP90 chaperone proteins, we found that ABA application to the DR_DU145 cell line led to the suppression of chaperone protein genes, particularly HSP70 and GRP94. This suppression allowed docetaxel to regain its cytotoxic effects against oxidative stress in the NR_DU145 cell line, thereby inducing apoptosis.

CONCLUSIONS

This study elucidates the role of ABA in modulating the expression of chaperone proteins, specifically HSP70 and GRP94, in the docetaxel-resistant prostate cancer cell line. Contrary to previous findings where ABA was shown to increase these chaperone proteins, herein we show that the application of ABA led to their suppression. This suppression enabled docetaxel to regain its cytotoxic effects against ER stress in the multidrug-resistant prostate cancer cell line, promoting apoptosis. These insights advance our understanding of the complex molecular mechanisms behind drug resistance in prostate cancer cells and underscore the potential therapeutic benefits of targeting chaperone proteins to overcome drug resistance.

Funding: This study originated from the corresponding author's PhD thesis and was supported by the Trakya University Scientific Research Fund (TUBAP 2017/223).

Acknowledgments: Thanks for all laboratory equipment supplied by the Department of Medical Biology, Faculty of Medicine, Trakya University; Zeynep Banu Doğanlar served as the thesis advisor.

Author contributions: Study design, investigation, data curation, writing/original draft preparation, review, and editing of the manuscript DŞ.

Conflict of interest disclosure: The authors declare that there is no conflict of interest.

Data availability: Relative gene expression calculations using one-way ANOVA with post-hoc Tukey's HSD and analyzed with SPSS statistical software are presented here: https://www.serbiosoc.org.rs/NewUploads/Uploads/Sumnulu,%20Raw%20Dataset.xlsx

REFERENCES

1. Bray F, Laversanne M, Sung H, Ferlay J, Siegel RL, Soerjomataram I, Jemal A. Global cancer statistics 2022: GLOBOCAN estimates of incidence and mortality worldwide for 36 cancers in 185 countries. CA Cancer J Clin. 2024;74:229-63. https://doi.org/10.3322/caac.21834
2. Pantziarka P, Capistrano R, De Potter A, Vanderborne L, Bouche G. An Open Access Database of Licensed Cancer Drugs. Frontiers in Pharmacology. 2021;12:627574. https://doi.org/10.3389/fphar.2021.627574
3. Luqmani YA. Mechanisms of Drug Resistance in Cancer Chemotherapy. Med Princ Prac. 2005;14:35-48. https://doi.org/10.1159/000086183
4. Persidis A. Cancer multidrug resistance. Nature Biotech. 1999;17:94-5. https://doi.org/10.1038/5289
5. Cortes JE, Pazdur R. Docetaxel. J Clin Onc. 1995;13:2643-55. https://doi.org/10.1200/JCO.1995.13.10.2643
6. Petrylak DP, Tangen CM, Hussain MH, Lara PN, Jr. Jones JA, Taplin ME. Docetaxel and estramustine compared with mitoxantrone and prednisone for advanced refractory prostate cancer. The New Eng J Med. 2004;351:1513-20. https://doi.org/10.1056/NEJMoa041318
7. Tannock IF, de Wit R, Berry WR, Horti J, Pluzanska A, Chi KN. Docetaxel plus prednisone or mitoxantrone plus prednisone for advanced prostatecancer. The New Eng J Med. 2004;351:1502-12. https://doi.org/10.1056/NEJMoa040720
8. Laurens V, Magadoux L, Isambert N, Plenchette S, Jeannin JF. Emerging targets to monitor and overcome docetaxel resistance in castration resistant prostate cancer. Int J Onc. 2014;45:919-28. https://doi.org/10.3892/ijo.2014.2517
9. Galletti E, Magnani M, Renzulli ML, Botta M. Paclitaxel and docetaxel resistance: molecular mechanisms and development of new generation taxanes. ChemMedChem, 2007;2:920-42. https://doi.org/10.1002/cmdc.200600308
10. Seruga B, Ocana A, Tannock IF. Drug resistance in metastatic castration-resistant prostate cancer. Nat Rev Clin Onc. 2011;8:12-23. https://doi.org/10.1038/nrclinonc.2010.136
11. Harris KA, Reese DM. Treatment options in hormone-refractory prostate cancer: current and future approaches. Drugs. 2001;61:2177-92. https://doi.org/10.2165/00003495-200161150-00003
12. Powles TJ. Evolving clinical strategies: innovative approaches to the use of mitoxantrone-introduction. Eur J Cancer Care. 1997;6(4):1-3. https://doi.org/10.1111/j.1365-2354.1997.tb00317.x
13. Rigacci L, Carpaneto A, Alterini R, Carrai V, Bernardi F, Bellesi G, Longo G, Bosi A, Rossi FP. Treatment of large cell lymphoma in elderly patients with a mitoxantrone, cyclo-

phosphamide, etoposide, and prednisone regimen: longterm follow-up results. Cancer. 2003;97:97-104. https://doi.org/10.1002/cncr.11032
14. Errington F, Willmore E, Tilby MJ, Li L, Li G, Li W, Baguley BC, Austin CA. Murine transgenic cells lacking DNA topoisomerase II b are resistant to acridines and mitoxantrone: analysis of cytotoxicity and cleavable complex formation. Mol Pharm. 1999;56:1309-16. https://doi.org/10.1124/mol.56.6.1309
15. Harker WG, Slade DL, Parr RL, Feldhoff PW, Sullivan DM, Holguin MH. Alterations in the topoisomerase II a gene, messenger RNA, and subcellular protein distribution as well as reduced expression of the DNA topoisomerase II b enzyme in a mitoxantrone-resistant HL-60 human leukemia cell line. Can Res. 1995;55:1707-16.
16. Harker WG, Slade DL, Drake FH, Parr RL. Mitoxantrone resistance in HL-60 leukemia cells: reduced nuclear topoisomerase II catalytic activity and druginduced DNA cleavage in association with reduced expression of the topoisomerase II b isoform. Biochemistry. 1991;30:9953-61. https://doi.org/10.1021/bi00105a020
17. Zhou R, Wang Y, Gruber A, Larsson R, Castanos-Velez E, Liliemark E. Topoisomerase II-mediated alterations of K562 drug resistant sublines. Med Onc. 1999:16(3):191-8. https://doi.org/10.1007/BF02906131
18. Bukowski K, Kciuk M, Kontek R. Mechanisms of Multidrug Resistance in Cancer Chemotherapy. Int J Mol Sci. 2020;21(9):3233. https://doi.org/10.3390/ijms21093233
19. Shinozaki K, Yamaguchi-Shinozaki K. Molecular responses to dehydration and low temperature: differences and cross-talk between two stress signaling pathways. Curr Opin Plant Biol. 2000;3:217-23. https://doi.org/10.1016/S1369-5266(00)80068-0
20. Schroeder JI, Kwak JM, Allen GJ. Guard cell ABA signalling and engineering drought hardiness in plants. Nature. 2001:410:327-30. https://doi.org/10.1038/35066500
21. Li HH, Hao RL, Wu SS, Guo PC, Chen CJ, Pan LP, Ni H. Occurrence, function and potential medicinal applications of the phytohormone ABA in animals and humans. Biochem Pharm. 2011;82:701-12. https://doi.org/10.1016/j.bcp.2011.06.042
22. Sakthivel P, Sharma N, Klahn P, Gereke M, Bruder D. ABA: a phytohormone and mammalian cytokine as novel pharmacon with potential for future development into clinical applications. Curr Med Chem. 2016;23:1549-70. https://doi.org/10.2174/0929867323666160405113129
23. Jung Y, Cackowski FC, Yumoto K, Decker AM, Wang Y, Hotchkin M, Lee E, Buttitta L, Taichman RS. Tumor removal limits prostate cancer cell dissemination in bone and osteoblasts induce cancer cell dormancy through focal adhesion kinase. Neoplasia. 2021;23:102-11. https://doi.org/10.1016/j.neo.2020.11.009
24. Zhou N, Yao Y, Ye H, Zhu W, Chen L, Mao Y. Abscisic-acid-induced cellular apoptosis and differentiation in glioma via the retinoid acid signaling pathway. Int J Can. 2016;138:1947-58. https://doi.org/10.1002/ijc.29935
25. Erdogan S, Doganlar O, Doganlar ZB, Serttas R, Turkekul K, Dibirdik I, Bilir A. The flavonoid apigenin reduces prostate cancer CD44+ stem cell survival and migration through PI3K/Akt/NF-κB signaling. Life Sciences. 2016;162:77-86. https://doi.org/10.1016/j.lfs.2016.08.019
26. Lockhart CA, Tirona RG, Kim RB. Pharmacogenetics of ATP-binding Cassette Transporters in Cancer and Chemotherapy. Mol Cancer Ther. 2003;2:685-98.
27. Sissung TM, Baum CE, Deeken J, Price DK, Aragon-Ching J, Steinberg SM, Dahut W, Sparreboom A, Figg WD. ABCB1 genetic variation influences the toxicity and clinical outcome of patients with androgen independent prostate cancer treated with docetaxel. Clin Cancer Res. 2008;14(14):4543-9. https://doi.org/10.1158/1078-0432.CCR-07-4230
28. Moreira JMA, Lima TS, Iglesias-Gato D, Souza LDO, Stenvang, Lima JDS, Røder MA, Brasso K. Molecular Profiling of Docetaxel-Resistant Prostate Cancer Cells Identifies Multiple Mechanisms of Therapeutic Resistance. Cancers. 2021;13:1290. https://doi.org/10.3390/cancers13061290
29. Llesuy SF, Arnaiz SL. Hepatotoxicity of mitoxantrone and doxorubicin. Toxicology. 1990;63(2):187-98. https://doi.org/10.1016/0300-483X(90)90042-F
30. Marzec M, Eletto D, Argon Y. GRP94: an HSP90-like protein specialized for protein folding and quality control in the Endoplasmic Reticulum. Biochim Biophys Acta. 2012;1823(3):774-87. https://doi.org/10.1016/j.bbamcr.2011.10.013
31. Amankwah YS, Collins P, Fleifil Y, Unruh, E, Márquez KJR, Vitou K, Kravats AN. Grp94 Works Upstream of BiP in Protein Remodeling Under Heat Stress. J Mol Biol. 2022;19:167762. https://doi.org/10.1016/j.jmb.2022.167762
32. Kadowaki H, Nishitoh H. Signaling Pathways from the Endoplasmic Reticulum and Their Roles in Disease. Genes. 2013;4:306-33. https://doi.org/10.3390/genes4030306
33. Kobayashi N, Takada Y, Hachiya M, Ando K, Nakajima N, Akashi M. Tnf-α Induced p21WAF1 but Not BAX in Colon Cancer Cells WiDr With Mutated p53: Important Role of Protein Stabilization. Cytokine. 2000;12:1745-54. https://doi.org/10.1006/cyto.2000.0782
34. Cho EK, Hong CB. Over-expression of tobacco NtHSP70-1 contributes to drought-stress tolerance in plants. Plant Cell Rep. 2006;25:349-58. https://doi.org/10.1007/s00299-005-0093-2
35. Volkov RA, Panchuk II, Mullineaux PM, Schoffl F. Heat stress-induced H2O2 is required for effective expression of heat shock genes in Arabidopsis. Plant Mol Biol. 2006;61:733-46. https://doi.org/10.1007/s11103-006-0045-4
36. Hu XL, Liu RX, Li YH, Wang W, Tai FJ, Xue RL, Li CH. Heat shock protein 70 regulates the ABA-induced antioxidant response of maize to combined drought and heat stress. Plant Growth Reg. 2010;60:225-35. https://doi.org/10.1007/s10725-009-9436-2

SUPPLEMENTARY MATERIAL

Supplementary Table S1. Gene codes and primer sequences for the qRT-PCR assay.

Genes	Primer Base Sequences
18S	F: GAGGATGAGGTGGAACGTGT R: GGACCTGGCTGTATTTTCCA
XBP1	F: TGGCCGGGTCTGCTGAGTCCG R: ATCCATGGGGAGATGTTCTGG
PERK	F: ATCCCCCATGGAACGACCTG R: ACCCGCCAGGGACAAAAATG
Ire1α (ERN1)	F: TGGGTAAAAAGCAGGACATCTGG R: GCATAGTCAAAGTAGGTGGCATTCC
EDEM1	F: CAAGTGTGGGTACGCCACG R: AAAGAAGCTCTCTCCATCCGGTC
HSP70	F: CGAGETCGACGCATTGTTTG R: GAGTGGATCCGCCGACGAGTA
GRP94	F: AATAGAAAGAATGCTTCGCC R: TCTTCAGGCTCTTCTTCTGG
p21	F: GGAAGACCATGTGGACCTGT R: GGCGTTTGGAGTGGTAGAAA
p53	F: CACGAGCGCTGCTCAGATAGC R: ACAGGCACAAACACACGCACAAA
ABCB1	F: TGCTGGAGCGGTTCTACG R: ATAGGCAATGTTCTCAGCAATG
BCRP/ABCG2	F: GGTGCCATTTACTTTGGGC R: ACAAAGAGTTCCACGGCTGA
MRP1	F: TGCCTTGGGATTTTTGCTGTG R: CGATCCCTTGTGAAATGCCC
MRP2	F: CTGCCTCTTCAGAATCTTAG R: CCCAAGTTGCAGGCTGGCC
MRP3	F: GATACGCTCACCACAGTCC R: CAGTTGCCGTGATATGGCTG
MRP4	F: CCTATGCCACGGTGCTGAC R: TGGCACATGGCTACTCGTAAC